ASSESSING USEFUL LIFE OF TURBOMACHINERY COMPONENTS

by

Murari P. Singh

President and Director of Technology

Safe Technical Solutions, Inc.

Bethlehem, Pennsylvania

Bhabesh K. Thakur

Senior Structural Analyst

and

William E. Sullivan

Senior Structural Analyst

GE Energy Conmec

Bethlehem, Pennsylvania

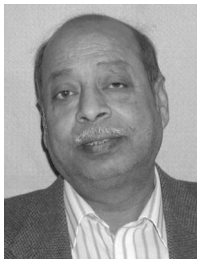

Murari P. Singh is President and Director of Technology for Safe Technical Solutions, Inc. (SafeTSol), in Bethlehem, Pennsylvania. He has been involved in the design, development, and analysis of industrial turbomachinery for more than 30 years at Turbodyne Corporation, Dresser Industries, Dresser Rand, and Conmec. Particularly, he has been involved with blade vibration, fatigue and fracture mechanics, stress and vibration of structure, reliability, life analysis, probabilistic analysis, FCC expanders, steam turbines, and centrifugal compressors. Dr. Singh has retired from GE Oil & Gas Conmec, where he was Chief Engineer and Manager of Engineering Technology.

Dr. Singh holds B.S., M.S., and Ph.D. degrees. He has authored more than 30 technical papers on a variety of topics related to turbomachinery.

Bhabesh K. Thakur is a Senior Structural Analyst at GE Power Systems, Oil and Gas, Conmec, in Bethlehem, Pennsylvania. He has more than 25 years of industrial experience that includes design, fabrication, testing, research and development, structural analysis, and project management. He is currently responsible for analysis, evaluation, and validation of turbomachinery component design.

Dr. Thakur received his BSME degree (1969) from RIT, Jamshedpur, India, MSME degree (1981) from Rochester Institute of Technology (1981), and Ph.D. degree (1986) from Rensselaer Polytechnic Institute.

William E. Sullivan is a Senior Structural Analyst with GE-Conmec in Bethlehem, Pennsylvania. His primary responsibilities include stress and vibration analysis of impellers, rotor blades, and bladed disk assemblies. Other duties include general structural analyses associated with rotating machinery and related hardware. Before joining Conmec in 1992, he was a Senior Engineer in the structures and dynamics group at Pratt & Whitney Aircraft, where he worked mostly on fan blade flutter testing and rotordynamics. Other experience includes various technical positions with the Combustion Turbine and Large Steam Turbine divisions of the Westinghouse Electric Corporation.

Mr. Sullivan has a B.S. degree (Engineering, 1977) from Widener University, and is a registered Professional Engineer in the State of Connecticut.

ABSTRACT

The last four or five decades have seen considerable advancements in the life assessment methods of mechanical components. These methods have been shown to be equally suitable for new as well as used components and even with components with discontinuities. Assessment of life of turbomachinery components has been done with the help of these methods. It will be demonstrated how one can use these methods to determine maintenance schedules. The same concepts also help to facilitate in repair or retire decisions of used components.

This tutorial discusses the utility of available and established techniques to perform life assessment of mechanical components. This will include the life assessment on the following basis:

- Deterministic type of assessment and
- Probabilistic type of estimation.

Presentation is arranged on the following topics:

- Discussion of common damage mechanisms,
- An overview of the concepts and the methods of life estimation, and
- Discussion of case histories extended to include the probabilistic aspect. Examples will include components from steam turbines, gas turbines, fluid catalytic cracking (FCC) expanders, and centrifugal compressors mostly taken from the literature where available.

INTRODUCTION

Traditionally, the reliability assessment of a component is based on the deterministic type of evaluation process. A component is considered reliable when a calculated factor of safety, i.e., implied margin of the design, is above certain predetermined value. Experience has shown that the component will work with these limit values. However, these methods do not provide the following important information.

- Most of these margins provide safety based on stress, i.e., the projected stress is kept below certain known material property. Determination about the safe operating life is difficult to ascertain by these numbers. The real issue, however, is to provide an answer to the question "what is the safe life of the component?"

• Deterministic methods do not consider variation and uncertainties in the value used for determining the margin.

This paper focuses on the discussion of tools that are available today that promise to bring a broader scope of data. This will permit industry to make a more quantifiable decision pertaining to the risk of continuing operation of machines or components.

These methods have helped in the process of making a decision about reliability, including retirement decisions and establishing maintenance and inspection intervals for turbomachinery. It will become evident that actual permissible variations rather than average worst case provide a more representative number for reliability. Examples are included to demonstrate the utility of the tools and the concepts. These have the promise to help in the life assessment of turbomachinery components on a logical and a rational basis. Therefore, statistical and probabilistic concepts will be discussed and used to assess the effect of variability present in geometrical dimensions, uncertainty in loads (operations), and variation in material properties.

Many of these topics have been presented, analyzed, and discussed by many but it seems prudent to review and discuss briefly some of the theory of probability, damage mechanisms, and concepts even at the risk of being repetitive and being perceived as recycling.

DETERMINISTIC TYPE OF ANALYSIS

In a deterministic type of analysis the estimated response of a mechanical component is kept below certain preestablished safe limits. The response may be deformation, strain, stress, etc. For example stress is kept below certain mechanical properties of the material of construction. A margin is usually allowed between the applied load (stress) and the established limit (strength of the material). One of such measures is known as "factor of safety." The desirability for use of the structure is signified by the value of factor of safety to be greater than unity.

In the deterministic evaluation of the reliability of a mechanical component, one assumes loads and material properties to be known and to be single valued. This process assumes no variation in them. Of course, the assumption that there is no uncertainty about them is hardly true in most of the practical applications.

PROBABILISTIC TYPE OF ANALYSIS

Due to uncertainty in the variables, the response is also expected to have scatter in its magnitude. Therefore, the estimated margin or "factor of safety" does not indicate true margin and does not indicate a good measure of safety. The estimation of the occurrence of the violation of the criteria or the "limit" is a measure of probability. Alternatively, the number of times response meets the criteria is a measure of probability of success, i.e., a measure of the reliability of the structure.

For example in a high cycle fatigue situation Goodman criterion is applied for reliability evaluation. The factor of safety is shown to depend on mean stress and alternating stress imposed on the component as well as on ultimate strength and fatigue strength of material of the component as it will be discussed in a later section. Uncertainty in the imposed loading and/or variation in the geometrical dimension of the component will be reflected in the magnitude of stress. Thus the stresses should be represented by a statistical distribution. Similarly the observed scatter in the material properties can also be described by statistical distribution. Once the scatter has been established then the chances of the factor of safety having a value larger than a desired value can be calculated, thus providing an estimate of probability.

Singh, et al. (2004), used the concept described above to estimate reliability of an impeller in the presence of a discontinuity. It was shown that the reliability of the impeller could be estimated with use of fracture mechanics. However, there are uncertainties or randomness in the parameters that can influence the reliability. For example there is scatter in the material properties and there is always uncertainty about the actual size of the defects. Singh (1991) also with the help of the fracture mechanic's concept and probabilistic methods evaluated reliability of a weld repaired steam turbine rotor. The life extension, remaining life assessment, and fitness-for-service concepts have evolved to keep plants running beyond design life. This has been achieved either by reassessing the design and/or repairing as needed. Methods using probabilistic concepts have been used to estimate reliability of many structures, e.g., Thacker, et al. (1990), used it for turbopump blades; Singh, et al. (Singh, 1985; Singh and Ewins, 1988; Singh, 1992), demonstrated its use for turbine blades and turbine bladed disk design.

The basic assumptions in each probabilistic evaluation are that with inherent variations in stress levels and in properties of the material, it is extremely rare that any particular set of values will occur at once. The limit values of each parameter might not occur at the same time. Once the statistical properties of any parameter influencing safe life of the equipment are known, the method allows us to estimate the probability of reaching a specific number of safe operating cycles.

The statistical property of any variable is described by a probability density function (PDF). Area under the curve is the probability of occurrence. By moving from left to right on the PDF, the probability of occurrences of a particular value increases.

Obviously, the more information one has on the statistical characteristics of the parameters used in estimating reliability, the better will be the estimate of the probability of reaching a specific number of cycles before failure. Analysis gets more complicated with an increasing number of parameters to be considered.

The response of a structure depends on the interaction of applied stress (S) and components' resistance (R). The deterministic method defines a margin by the ratio R/S, called factor of safety. There are uncertainty in the values of both S and R and these are represented in statistical terms by a PDF. In the probabilistic terms the reliability is estimated as follows:

$$P_f = P(R < or = S) \tag{1}$$

where P_f is the probability of failure.

Figure 1 shows graphically the mathematical statement made by Equation (1). The shaded portion under the curve is not considered in the deterministic evaluation.

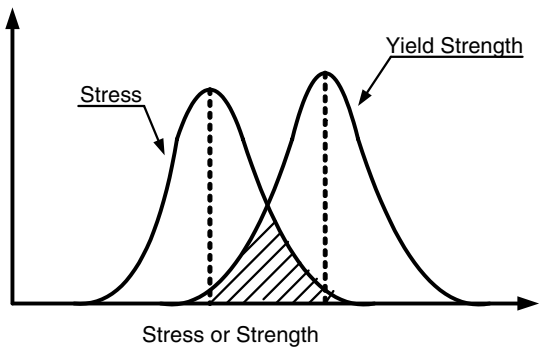

Figure 1. Description of P_f = P((R-S) < or = 0).

Even for a simple case, calculation can get very involved. To mitigate this complexity, techniques have been developed that perform many calculations (often thousands) rapidly or at least automatically using information from PDFs. In Monte Carlo simulation, for example, by using multiple analyses a picture of the probability of safely achieving any number of operational cycles immerges. Using the results of such a simulation, the level of risk associated with any given cycle to failure can be established. Based on this information, better decisions can be made using an estimated risk for operating the equipment with a suspected flaw, but the risks associated with reaching a particular number of cycles can be ascertained as well.

DAMAGE MECHANISMS

Damage of a component will be considered as the inability of the component to perform its intended function reliably, economically, and safely. Specifically, damage manifests itself as:

- Excessive deformation (a deformation failure is a change in the physical dimensions or shape of a component that is sufficient for its function to be lost or impaired),
- Breakage of parts in just a single application of load (may result in multiple pieces),
- Breakage or undesirable deformation after some elapsed time under sustained loadings (creep rupture),
- Breakage due to fluctuating load (may result in multiple pieces, high cycle fatigue (HCF) or low cycle fatigue (LCF), interaction of HCF, LCF, and creep),
- Fracture in the presence of discontinuity in the material (may result in multiple pieces, crack growth, fracture mechanics).

The following mechanisms will be discussed and examples of the methods for assessing the effect of each of the mechanisms will be provided in later sections. In particular these mechanisms are:

- Creep
- High cycle fatigue,
- Low cycle fatigue,
- Fatigue-creep interaction, and
- Growth of a discontinuity in the material.

DEFORMATION

Deformation or strain (deformation per unit length) is a measurable quantity and damage is inferred through the knowledge of deformation and theoretically by strain. Stress is conventionally used to define the limit for safe use of a mechanical component. Stress is an inferred quantity because it is derived from measured displacement or strain. Stress is never measured. Importance of this argument will become clear by examining the material data from the basic pull test, i.e., stress-strain curve, shown in Figure 2.

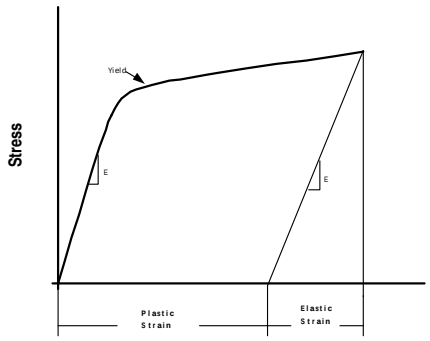

Figure 2. Typical Stress Versus Strain Curve for a Metal.

Deformation or strain can be classed as either elastic deformation or plastic deformation. Elastic deformation is recovered upon unloading. Where this is the only deformation present, stress and strain are proportional for most materials. For axial loading, the constant of proportionality is the modulus of elasticity, E.

Plastic deformation is not recovered upon unloading and is therefore permanent. Once the plastic deformation begins, only a small increase in stress usually causes a relatively large additional deformation. The value of stress where this behavior begins is called yield strength.

It is the plastic or in general terms the inelastic strain that causes damage in the material. The sustained type (steady) of loading that causes yielding becomes undesirable. If the load is kept on, material can go to final fracture. In the case of variable loads, the strains that are not recovered provide energy for the damage in material. Generally, ductile materials are able to sustain large strains compared to brittle materials.

THEORIES OF FAILURES FOR STATIC LOADING

Many theories have been propounded to estimate the maximum static load that may be applied to a component without causing failure. These theories use data obtained from uniaxial tests when in the real situation the stress system will be multiaxial. This way one can avoid experimental determination of an infinite number of stress combinations of stresses that may arise in the real situation. Some of them are listed below. A more detailed description is provided in APPENDIX A.

- Maximum Normal Stress Theory (Rankine Theory)
- Maximum Normal Strain Theory (Saint Venant Theory)
- Maximum Shearing Stress Theory (by Guest)
- Internal-Friction Theory and Mohr Theory (by Coulomb and Mohr)
- Maximum Strain Energy Theory (by Beltrami, by Huber, by Haigh)
- Hencky-von Mises Theory (by Hencky and by von Mises)

In a uniaxial tension test, when the specimen starts to yield, the following six quantities reach their limits simultaneously:

1. The principal stress ($\sigma = P/A$) reaches the tensile elastic strength (elastic limit or yield point) of the material.
2. The tensile strain ε reaches the value of strain, ε_e.
3. The maximum shearing stress ($\tau = \frac{1}{2} P/A$) reaches the shearing elastic limit or shearing yield stress τ_{yp} of the material, $\tau_{yp} = \frac{1}{2}\sigma_{yp}$.
4. The total strain energy W absorbed by the material per unit volume reaches the value $W_e = \frac{1}{2} (\sigma^2 e/E)$.
5. The strain energy of distortion W_d (energy accompanying change in shape) absorbed by the material per unit volume reaches a value $W_{de} = ((1+\mu)/3E)\ \sigma_e^2$.
6. The octahedral shearing stress reaches the value $\tau_{Ge} = (\sqrt{2/3})\ \sigma_e = 0.47\ \sigma_e$

In the case of a uniaxial tensile test each of the six quantities described above are reached simultaneously. When the state of stress is multiaxial the listed six quantities will not occur simultaneously. It becomes important to consider which one of the quantities should be chosen to limit the loads that can be applied to a member without causing inelastic strain.

DETERIORATION MECHANISM

Creep

A permanent deformation can also occur when a high loading is applied and is maintained constant for some time. This phenomenon of permanent set, which is time dependent, is called creep. This type of permanent deformation occurs in materials at high temperature even at a relatively low stress. If the load is applied for a longer period of time, the component can also rupture. This is termed stress rupture.

Creep properties are generally determined by means of a test in which a constant axial load or stress is applied to the specimen and resulting strain is recorded as a function of time. After the instantaneous strain, ε_o, a decelerating strain rate stage (primary creep) leads to a steady minimum creep rate, $\dot{\varepsilon}$ (secondary creep), which is finally followed by an accelerating stage (tertiary creep) that ends in fracture at a time, t_r. The strain at rupture, ε_r, represents the rupture ductility. Larson and Miller (1972) introduced a very

useable concept of a time-temperature parameter in the form T(C + log t). Their argument depended on the rate theory. This parameter is known as the Larson Miller Parameter (LMP). The result of this method is to collapse a large amount of data to a single curve. Thus a plot of stress versus LMP results in a single plot, within limit of scatter, regardless of the time-temperature combination employed to drive the parameter. A value of 20 was initially proposed for C, but a value between 10 and 40 is found to be suitable for many materials. T is taken in absolute units (°F + 460) and time in hours. A typical chart for a material is shown next in Figure 3.

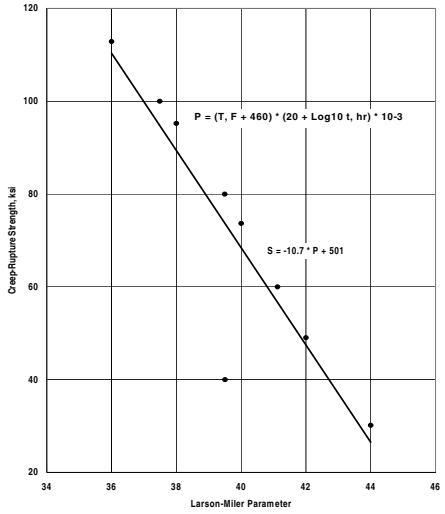

Figure 3. Larson-Miller Parameter Chart for Waspaloy®.

In a general term the following equation is used:

$$Stress = Function\ of\ (LMP), \tag{2}$$

where LMP = $(T + 460)(20 + \log_{10} t).10^{-03}$.

It is evident from Equation (2) that when stress and temperature are known, the time to rupture can be estimated. In the case for a required life of the component at a given operating temperature, the limit on the applied stress can be found. This is a deterministic evaluation without any regard of variations in either of the parameters. Examine Figure 4, which shows variations in applied stress as statistical distribution and upper and lower limit curves representing scatter in the test data.

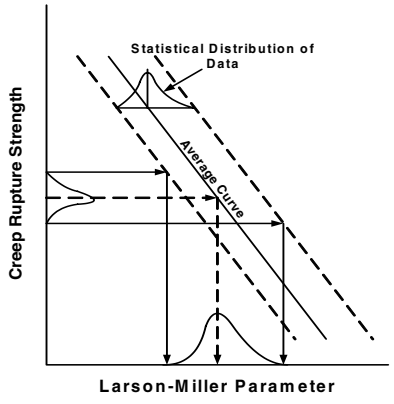

Figure 4. Probabilistic Type Plot of Creep Rupture Data.

Figure 4 pictorially shows the variation in the estimated LMP. This scatter will result in a statistical type distribution on life for given temperature. Later an example will be provided that will show the difference between two approaches (deterministic and probabilistic) and the implication on the design decision.

HIGH CYCLE FATIGUE

If the number of cycles to failure for a mechanical structure is large under cyclic load with relatively small stress, it is known as high cycle fatigue. The most widely used design criterion in a high cycle fatigue situation is called Goodman criterion. This is depicted on a Goodman diagram. The cyclic material properties used in this diagram is taken from stress (S) versus cycles to failure (N) data obtained from laboratory tests on the material (Figure 5). The slope of this curve for most materials is almost horizontal after about 10^6 cycles. Below the corresponding stress level of 10^6 cycles, a small reduction in stress produces a large increase in life. A component's health is determined by a factor of safety that is calculated by an equation proposed by Goodman. Just the knowledge of this calculated factor of safety, however, does not provide any clue about the expected life of the component. A method has been proposed by Singh (2001) to calculate a factor of safety based on life.

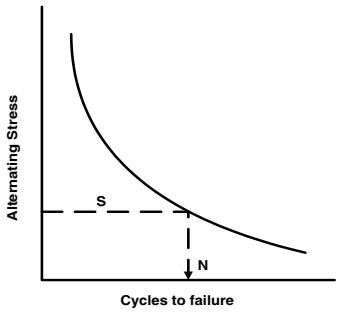

Figure 5. S-N Curve.

Mean stress influences the fatigue life of a mechanical component. The Goodman equation accounts for the effect of mean stress on fatigue life and it is given below:

$$\sigma_a / \sigma_e + \sigma_m / \sigma_{ult} = 1 / FS \tag{3}$$

Equation (3) represents a straight line as shown in Figure 6 for factor of safety (FS) equal to unity. Each radial line of Figure 7 corresponds to a life and it represents the magnitude of fatigue strength, i.e., the magnitude of alternating stress when the mean stress is zero for a given life as depicted in the S-N curve.

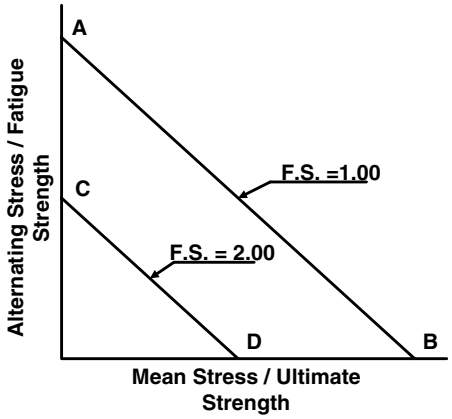

Figure 6. Goodman Diagram with Factor of Safety Line.

When a mechanical structure goes through a complete cycle of loading, the total strain of the hysteresis loop consists of two parts, namely elastic strain and inelastic strain. Figure 8 shows an ideal hysteresis loop representing one cycle of a cyclic loading.

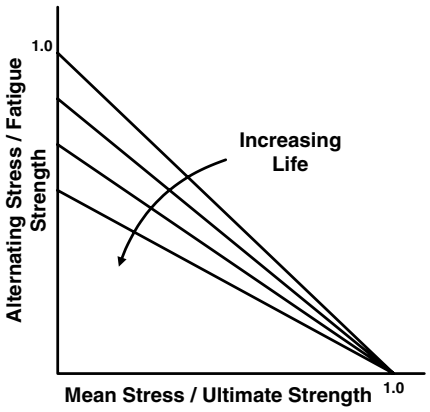

Figure 7. Goodman Diagram with Constant Live Lines.

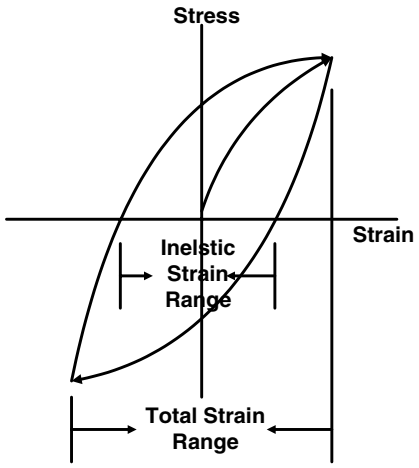

Figure 8. An Ideal Hysteresis Loop.

In general, however, the inelastic strain is composed of plastic strain and creep strain. For pure fatigue loading, creep strain is zero, thus the inelastic strain is composed of only plastic strain.

Total Strain = Elastic Strain + Plastic Strain

$$\begin{aligned} \Delta\varepsilon_{total} / 2.0 &= A N_f^b + C N_f^d \\ &= \left(\sigma_f^{'} / E\right) N_f^b + C N_f^d \end{aligned} \tag{4}$$

Morrow (1965) modified the above equation as shown below to include the effect of mean stress on cycles to failure as follows:

$$\Delta\varepsilon_{Total} / 2.0 = \left(\left(\sigma_f^{'} - \sigma_m\right) / E\right) N_f^b + C N_f^d \tag{5}$$

The first of the above equations relates to the HCF part of the life estimation while the second part relates to the LCF.

Singh (2001) derived an expression for cycles to failure for a specified factor of safety (FS):

$$N_f = \left(\left(1 / FS - \sigma_m / \sigma_{ult}\right)\left(\sigma_e / \left(\sigma_f^{'} - \sigma_m\right)\right)^{(1/b)}\right) \tag{6}$$

where N_f is the cycles to failure for a given FS. This is a function of FS, σ_m, and material properties.

PROBABILISTIC HCF

By applying the above equations, Singh (2001) demonstrated the probabilistic reliability assessment of mechanical components. Figure 9 helps explain the reasoning behind such evaluation. It shows an S-N diagram of a material with a band of curves. The band represents the scatter of the test data. The estimated stress applied to a component is also shown to have variation on the y-axis. This variation results from the influence of variations in operating loads, geometrical tolerances, and it also includes the inaccuracy in the calculation method.

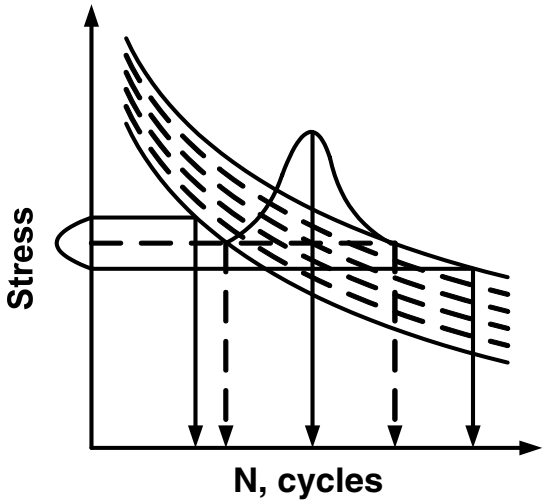

Figure 9. Depicting Scatter of Data in S-N Curve.

The resulting assessment of the operating life is shown on the x-axis. It is clear that due to variations in material property and stress, the operational cycle is not single valued but it varies within a range. The implication of this can be seen in the probabilistic Goodman diagram shown in Figure 10. The factor of safety is not single valued but has a range of values; therefore operating life will also have a range.

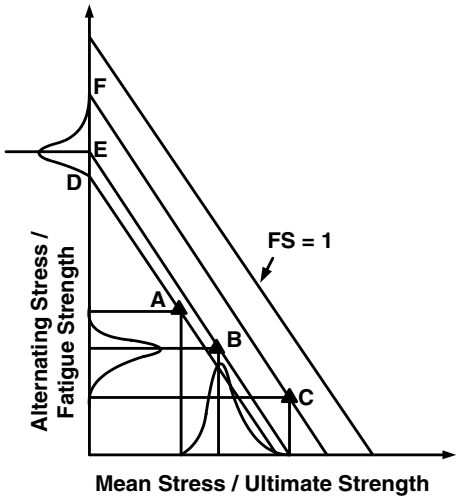

Figure 10. A Probabilistic Aspect of Goodman Diagram.

LOW CYCLE FATIGUE

When the cyclic stresses are high, typically in the neighborhood of the yield strength of the material, the applied load cycles to failure are small. The life is controlled by the inelastic component of strain. The total strain has elastic and inelastic components, and the plots of these components versus cycles to failure on a log-log plot are straight lines.

The most widely quoted fatigue life model is often expressed by the Mason-Coffin equation relating life to plastic strain range through a power law. Manson and Halford (1967) proposed that the cyclic life depended on total strain range, which in turn consisted of elastic and plastic components, each of which was linear with

cyclic life on log-log scales. Total strain range was thus asymptotic to plastic line in the LCF region where plastic strain was much larger than elastic strain, and asymptotic to the elastic line in the HCF range where the elastic strain greatly exceeds plastic strain.

$$\begin{aligned}\Delta\varepsilon &= \Delta\varepsilon_p + \Delta\varepsilon_e \quad = \Delta\varepsilon_p + \Delta\sigma / E \\ &= MN_f^Z + (G / E)N_f^Y\end{aligned} \tag{7}$$

The coefficient M is primarily governed by ductility, and coefficient G by strength.

Low cycle fatigue tests are time consuming and expensive as compared to monotonic tensile tests. Halford and Manson (Halford and Manson, 1968; Manson and Halford, 1967) proposed the method called Universal Slope after examining the properties of a large number of materials. By utilizing monotonic tensile properties, a strain versus cycles to failure curve can be estimated. This method does not give the most accurate results for all materials, but it provides a very good first estimate. To aid in the material testing for fatigue and initial comparison among materials, this method has been found to be very useful. They realized that to obtain fatigue properties of material is time consuming and expensive. They tried to use monotonic test properties to estimate fatigue properties. A simple equation universalizing the life model exponents with an approximate relation of M and G to the material properties was proposed:

$$\Delta\varepsilon = D^{0.6}N_f^{-0.6} + (3.5\sigma_u / E)N_f^{-0.12} \tag{8}$$

where D is the logarithmic ductility and σ_u the ultimate tensile strength, and E the elastic modulus. An example chart for SS347/348 bar at 1000 F is shown in Figure 11.

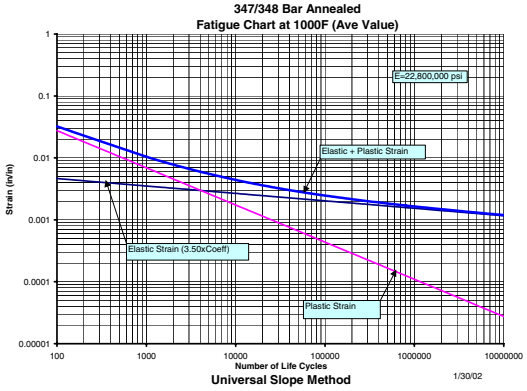

Figure 11. Life Cycle Chart for SS347/348 Bar Using Universal Slope Method.

Morrow (1965) arranged the life relation equation as follows:

$$(\Delta\varepsilon)/2 = \varepsilon_f (2N_f)^c + (\sigma_f / E)(2N_f)^b \tag{9}$$

where strain is expressed as amplitude, rather than a range, and life as a reversal (a cycle being two reversals). ε_f is defined as a "ductility coefficient," and σ_f as a strength coefficient. He also modified the equation to include effect of mean stress on the fatigue life of the component as discussed earlier.

The probabilistic discussion for the LCF life assessment is the same as for the HCF. Due to uncertainties in the involved parameter the LCF life will also have a range with different probabilities associated with it. An example that provides support to the above argument is given later.

FATIGUE AND CREEP INTERACTION

In the event a component is subjected to a cyclic load with a possibility of creep deformation in the material during cycling, fatigue and creep interaction may occur. The phenomena of fatigue and creep interaction are complex. Many methods of treating this phenomenon have been proposed; a large number of which are similar. In each case, there is a basic link in the framework of the method to one or more of the mechanisms that is relevant to the high temperature problems. Some of them are listed below.

- Time and Cycle Fraction Summation (Robinson, 1952; Taira, 1962)
- Ten Percent Rule (Halford and Manson, 1968; Manson, 1966; Manson and Halford, 1967)
- Time and Cycle Fraction Summation Using Cyclic Creep Rupture Data (Manson, et al., 1971)
- Frequency Modified Life Equation (Coffin, 1971)
- Strain Range Partitioning Method (Manson, et al., 1971)
- Frequency Separation (Coffin, 1976)
- Hysteresis Loop Analysis (Ostergren, 1976)
- Energy Based Analysis (Leis, 1977)
- Damage Accumulation (Majumdar and Maiya, 1976, 1979, 1980)

Manson (1971) proposed the method of strain range partitioning (SRP). Over the past many years, many materials have been tested using the SRP framework and laboratories in other countries have investigated its usefulness in relation to their problems. In 1978, a NATO AGARD meeting was held in Aalborg, Denmark, specifically for the purpose of sharing experiences among the U.S. and European laboratories in the application of this method given in the literature ("Characterization of Low Cycle High Temperature Fatigue by the Strainrange Partitioning Method," 1978).

While some limitations were recognized, the general usefulness of the approach was verified. More recently the method has been evaluated in Japan, and at least one investigative team (Hirakawa and Tokimasa, 1981) expressed SRP to be "…the most promising of the methods studied…" for the types of materials used. Thus, the basic concepts behind SRP (both a scientific explanation of material behavior and a technologically viable method) have been examined and verified by many investigators.

The major portion of the following description has been taken from the work of Manson and Halford (1983). Further discussion will be limited to the strain range partitioning method.

SRP METHOD

The basic thrust of this method is that different types of strain range type yield different hysteresis loops, thus it should yield different life.

The SRP method attempts to take cognizance of two types of deformation that can occur in the creep range for some materials. The strain that is introduced by grain boundary (GB) sliding and attendant slip plane (SP) sliding is referred to as "creep." On the other hand, if the loading is rapid, there is no time for GB sliding to occur, and all strain is absorbed as SP sliding such as plasticity occurs at room temperature by only SP sliding without involvement of GB sliding. For this reason, the strain introduced by SP sliding will be called "plasticity" even if it occurs at high temperature.

Four different types of strain ranges become possible by combining the two types of strains with their occurrence in the tension and compression halves of the loop. "Plastic" and "creep" strain are referred to as P and C, and the notation that the first letter refers to the tensile part of the loop and the second to the compressive half is adopted. The four permutations of strain ranges that are possible become ε_{pp}, ε_{cc}, ε_{cp}, and ε_{pc}.

The other types of strain range involve different types of combined slip plane and grain boundary sliding, producing different deformation effects and life relationships. An overall

view of the four types of strain range and the idealized associated hysteresis loops are shown in Figure 12.

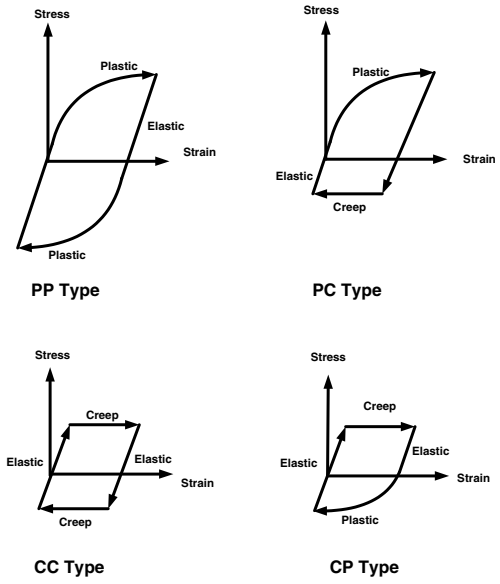

Figure 12. Types of Deformation That Can Occur in the Creep Range.

The level of damage due to cyclic loading, i.e., due to fatigue of a component, should be proportional to the area of the hysteresis loop created during cyclic loading. Experimental results show that even for the same strain range life can be different for different strain types (Figure 13).

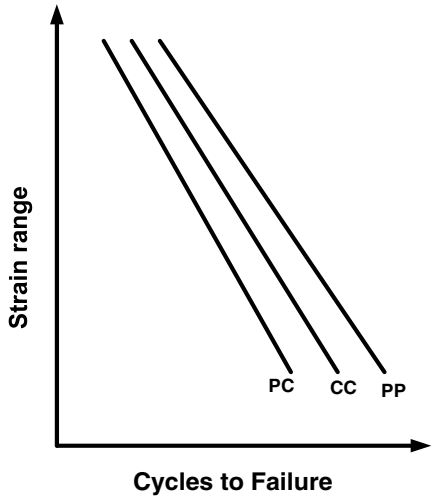

Figure 13. Strain Range Versus Cycle Curves for PP, PC, CC Types.

It seems that the following are the two main reasons for the appeal for the use of SRP.

- SRP provides a mechanism for the use of simple cyclic test data (similar to the use of uniaxial test data in the case of multiaxial stress system) to complex cyclic hysteresis loops in the event of creep fatigue interaction.
- Life should depend on the type of strain even though the magnitude of strain range may be identical.

Vogel, et al. (1976), used the SRP method to predict crack initiation life of a jet engine's combustor liner and correlated the analytical results against representative engine and test rig data. They concluded that the SRP approach with the calculated stress/strain presented in the paper is a viable method for predicting combustor chamber liner life to a cracking mode of failure. Moreno, et al. (1983), compared results of two analyses, one from SRP and the other from a method produced by a major turbine manufacturer. The life was overpredicted by analyses compared to the observed cyclic crack initiation life. McKnight, et al. (1983), used the SRP method to predict crack initiation life. The SRP method predicted life from 1200 to 4420 cycles compared to an observed life of 3000 cycles. Schiffer, et al. (1990), and Lucas and Singh (1992) described the use of SRP technique in the design of components for a compressed air energy storage (CAES) expander.

CUMULATIVE FATIGUE DAMAGE ANALYSIS

Damage to material is a nonreversible and a nonlinear process. The linear type of cumulative damage rule has been widely used but this could not take into account the effect of sequence of loadings. Phenomenon of damage is path dependent because it is a nonlinear process. The situations arise where many hystensis loops of different types are imposed on a given structure. A cumulative damage analysis is required to take into account the fatigue damage done by hysteresis loops representing different load histories. Practical cases are encountered where high cycle fatigue and low cycle fatigue are superposed having large differences in amplitude and frequencies. To analyze such a situation Manson and Halford (1981) developed the damage curve approach (DCA). In a situation when many different types of load history can be imposed on a structure, the DCA lends to clean calculation strategy and the method can be automated.

Figure 14 helps in understanding the approach. This plots the accumulation of "damage" as a function of cycle ratio for various life values. The linear damage rule would require that the curves be coincident for all life level. It is their separateness that produces the loading order effect. All curves start at the origin that represents the initial condition of the material where the damage state is zero, and terminates at failure F where D = 1.0.

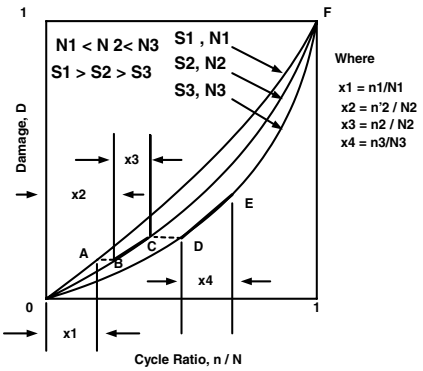

Figure 14. Damage Curve Concept for Cumulative Damage in Complex Loading.

The DCA concept is that damage accumulation proceeds along the curve associated with the life level at which a cycle ratio is applied. For example if a cycle ratio n_1/N_1 is first applied at the life level N_1, the damage will go from zero to A. If at this point a new loading level is introduced, the life of which is N_2 and the damage curve is OBF. The point B on this curve has the same damage as point A on curve OAF. If n_2 cycle is then applied at the N_2 life level, the point C is located as shown. Similarly, if n_3/N_3 is applied at the N_3 life level, point D is located at the same level as C and increment DE by the cycle ratio n_3/N_3 and so on for an arbitrary sequence of loading.

The extent of the loading order effect is shown in Figure 14. In a two level test at which the first load is applied at the low life

level, say from O to A followed by a loading at a higher level, say from B to F, the sum of the cycle ratio clearly omits the distance AB and is less than unity. If the high life cycle ratio is applied first along OB followed by the low life cycle ratio along AF, it is clear that the cycle ratio associated with AB is included twice, and therefore the summation of the cycle ratio is greater than unity. They defined damage (D) as:

$$D = \left(1/a_f\right)\left(a_0 + \left(a_f - a_0\right)\left(n/N_f\right)^{(2/3)^{N_f^{0.4}}}\right) \tag{10}$$

In a more general case when K loadings are applied before failure occurs, the equation for DC analysis becomes:

$$\left(\left(\left(n_1/N_1\right)^{\left(N_1N_2\right)^{0.4}} + n_2/N_2\right)^{\left(N_2N_3\right)^{0.4}} + n_s/N_3\right)$$
$$\left(\left(N_3/N_4\right)^{0.4} + \ldots + n_{(k-1)}/N_{(k-1)}\right) \tag{11}$$
$$\left(N_{K-1}/N_k\right)^{0.4} + n_k/N_k = 1$$

Subscripts 1, 2, 3, … (K−1), K are sequence numbers of the loadings as they occur. Of particular interest in Equation (11) is that the only constant that remains in the final equation is the exponent 0.4; all the others cancel in the derivation. Examination of a series of values in the range of 0.3 to 0.5 reveals that the final result is not greatly altered when one uses 0.4. The use of Equation (11) was suggested based on universalized value of 0.4 as the exponent.

The SRP method in general can be utilized to estimate life in the situation of fatigue creep interaction by following the steps listed below:

- Material is tested to generate strain range versus life data for the basic pure generic strain types.
- The effect of the operational load histories is estimated by analysis. From the resulting hysteresis loops tabulation is made of the estimated various types of strain ranges for each operational cycle type.
- Prediction can be made regarding the number of cycles to failure for each load history by using the interactive damage rule.
- The damage curve analysis technique is used to assess the life of the component by combining different load histories.

FRACTURE MECHANICS

The presence of a crack or crack like discontinuity may weaken a component. Crack might grow to failure so that it fractures into two or more pieces. This can occur even at stresses below the material's yield strength. Many books and technical papers (Hertzberg, 1965) have been written about the practical use of fracture mechanics. For more detailed descriptions, the references mentioned earlier should be studied. The objective of this section, however, is to provide and discuss some salient features briefly about the subject. This is important so that one can appreciate the theory and the analysis process to be used later in this paper. Emphasis is placed on the basic principles with the fracture mechanics model that can be used in making decisions about reliability of components with reportable discontinuities. Two more important aspects were discussed in Singh (2004) as listed below:

- Basic assumptions to understand the theoretical framework
- Aspects of fracture theory to establish a physical basis for design of mechanical structure

In the fracture mechanics type of analysis, the stress fields near the crack tips are classified as three basic types. These are shown in Figure 15. Mode I is called opening mode, Mode II is known as sliding mode, and Mode III is termed as tearing mode. Of all three modes, Mode I is the most pertinent for brittle crack propagation.

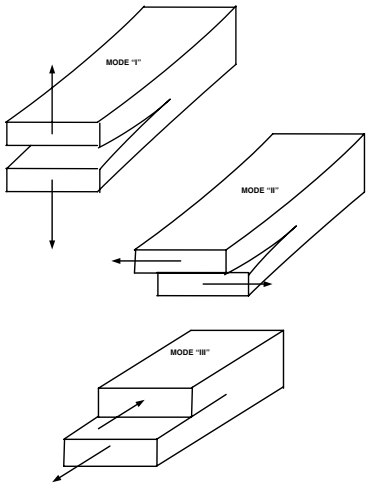

Figure 15. Modes of Fracture.

The stress distribution near the crack tip is analyzed by use of the theory of elasticity. The analysis is simplified based on the sharp slit approximation of a crack (Figure 16), the tip of the crack is assumed to be perfectly sharp in the unstressed condition. The surfaces generated by moving cracks are considered to be free of forces at all stages of loading. The stress field at the crack tip takes a simple solution of stress field near the tip (the distances from the tip are small compared to the characteristic dimensions of the crack system).

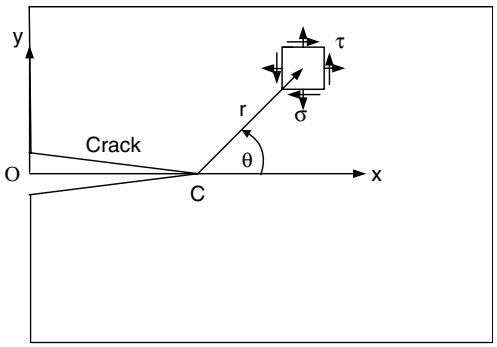

Figure 16. Stress Analysis at the Crack Tip.

The characteristics of the stress field and its strength at the crack tip are defined by the stress intensity factors (K_I, K_{II}, K_{III}). It depends only on the loading and crack geometry. The stress intensity factor is the mathematical expression that describes the redistribution of load paths for transmitting load past a crack.

$$K_I = \left(1.21\pi a\right)^{1/2}\left(\sigma\right)$$
$$\Delta K_I = \left(1.21\pi a\right)^{1/2}\left(\Delta\sigma\right) \tag{12}$$

An expression for the crack growth rate (called slow crack growth regime) versus alternating stress intensity factor is expressed as follows:

$$da/dN = m\left(\Delta K\right)^b \tag{13}$$

or

$$\log\left(da/dN\right) = \log\left(m\right) + b\ \log\left(\Delta K\right) \tag{14}$$

The plot of the above expression on a log-log plot is a straight line with b as the slope of the straight line. A similar equation generated from the material test data has been used to assess reliability of many mechanical components for many years.

A reliability evaluation of a mechanical component can be accomplished with the following information:

- Location, size, and orientation of indication
- Far field stress near the indication
- Analytical expression of the stress intensity factor at the crack tip, e.g., the crack tip stress intensity factor of a surface crack with a circular cross section is expressed as:

$$K_I = (1.21\pi a)^{1/2}(\sigma) \tag{15}$$

- Estimation of cycles required for the initial crack (a_i) to reach the critical crack size (a_c) is derived from the equation representing crack growth data [Equation (13)]:

$$N = \left(a_f^p - a_i^p\right) / \left((1.21\pi)^{0.5b}\, pm(\Delta\sigma)^b\right) \tag{16}$$

And the final crack length after N cycles is given by:

$$a_f = \left(a_i^p + (1.21\pi)^{0.5b}\, pm(\Delta\sigma)^b N\right)^{1/p} \tag{17}$$

where p = (2.0−b)/2.0.

- Material properties are obtained by appropriate fracture mechanic type tests.

PROBABILISTIC ASPECT

As discussed earlier due to scatter in the material data and/or uncertainty in stress estimation and physical dimensions thereby causes variation in the ΔK. Figure (17) shows the scenario where the da/dn values and in the end the estimated life (N) will have variability. There are ways to estimate that variation in terms of statistical distribution that will yield a reliability curve for N. This will be demonstrated by example.

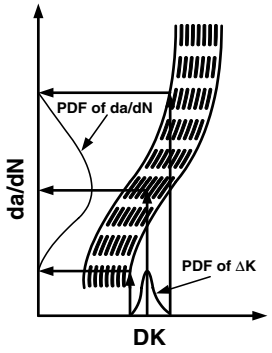

Figure 17. Probabilistic Aspect of Crack Growth Data.

EXAMPLE 1— CREEP RUPTURE LIFE EVALUATION OF A MECHANICAL COMPONENT

To illustrate the use of the Larson-Miller parameter (LMP) and a deterministic approach this example is taken from Viswanathan (Undated). This can represent any component at high temperature and effect on creep life due to change in temperature. Under design condition of stress, σ = 7.5 ksi, and temperature, T = 1000°F, design is good for 347,520 hours (40 years) based on the creep property of the material of construction. Later on the plant is to be operated such that the temperature, T, of the component will be estimated to be 1050°F. Assessment is made in the resulting reduction of creep life of the component using the Larson-Miller parameter.

- T = 1000°F

t = 347,520 hours

LMP = (T + 460)(20 + $\log_{10}$ t) = 37,289

As LMP is a function of stress and stress has not changed, LMP will remain the same.

Now, for T = 1050°F and for the estimated LMP:

- (1050 + 460)(20 + log t) = 37,289 or

t = 49,573 hours (5.7 years)

The estimated reduction in creep life of the component life is:

- 347,520 hours − 49,573 hours = 297,947 hours (34.3 years)

Assume a 4 percent spread in temperature, i.e., from 1029°F to 1071°F (2 percent variation on either side of 1050°F) in the estimate and it is normally distributed. A probabilistic calculation using a Monte Carlo simulation is done for the percent probability of achieving creep life. It is shown in Figure 18 and Figure 19. Table 1 lists the calculated probability associated with a desired creep rupture life of the component. It is evident from Figure 19 that after including the influence of variations in parameters, a creep rupture life of about 3.5 years with a probability of 99.98 percent is achievable. However, there is only 49.98 percent probability of achieving a creep rupture life of 5.7 years as estimated by the deterministic approach.

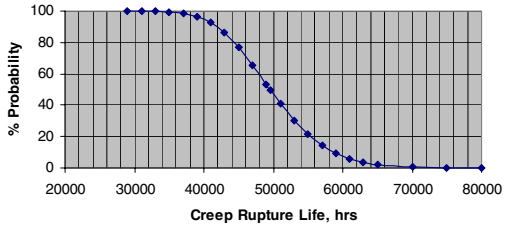

Figure 18. Creep Rupture Life (Hours) Versus Percent Probability.

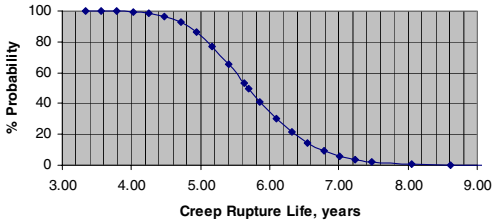

Figure 19. Creep Rupture Life (Years)Versus Percent Probability.

EXAMPLE 2— LCF LIFE EVALUATION OF A MECHANICAL COMPONENT

This example demonstrates the method of assessing LCF life of a component. The use of the cycle versus strain amplitude relation to determine the life of an intake assembly for a hot gas expander based on the finite element analysis (FEA) result is illustrated next.

The normal operating conditions data for the example case are as follows:

- Inlet temperature: 1400°F
- Discharge temperature: 1150°F
- Nosecone flange inner ring temperature: 800°F

The following loading conditions are considered for this:

- Mechanical loads—pressure, gravity, and piping
- Thermal loads with temperature gradient of 1400°F/1100°F at intake flange and 1400°F/800°F at nosecone flange

Table 1. Creep Rupture Life Versus Percent Probability.

Creep Hrs	Creep Life, Yrs	% Probability
80000	9.20	0.013
75000	8.62	0.092
70000	8.05	0.45
65000	7.47	2.02
63000	7.24	3.44
61000	7.01	5.77
59000	6.78	9.35
57000	6.55	14.42
55000	6.32	21.48
53000	6.09	30.45
51000	5.86	41.34
49573	5.70	49.94
49000	5.63	53.44
47000	5.40	65.58
45000	5.17	76.86
43000	4.94	85.98
41000	4.71	92.61
39000	4.48	96.68
37000	4.25	98.73
35000	4.02	99.61
33000	3.79	99.91
31000	3.56	99.98
29000	3.33	100

A life cycle chart is shown in Figure 20 and the FEA model for the component is shown in Figure 21.

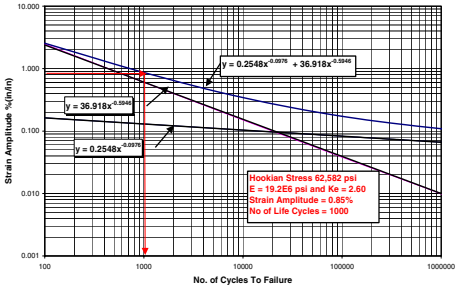

Figure 20. Life Cycle Chart for SS347/348 (0.004 In/Sec) Based on Test Data. (Courtesy Conway, et al., 1975)

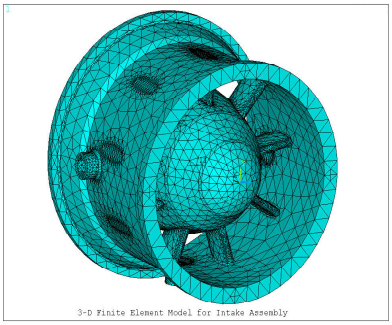

Figure 21. FEA Model for the Example Intake Assembly.

The FEA was performed with the loadings described earlier. The analysis considered elastic deformation only. The estimated maximum stress is about 62,600 psi, which is larger than the yield strength of the material of construction. It means that for the loading considered, there might be plastic localized deformation in the structure. Thus, the result either should be adjusted for the plastic deformation or an elastoplastic analysis should be conducted. The result of the analysis for mechanical as well as thermal loads is shown in Figure 22. The elastic analysis yields stress value larger than actual and the corresponding strain values to be lower than the actual value. It is the value of strain that should be considered for the life calculation. For this analysis adjustment is made by using Neuber's approximation, which has been used successfully in cases of localized yielding. The total strain is estimated to be about 0.85 percent for the stress value of 62,600 psi. The corresponding plastic strain is about 0.60 percent. Following is a brief description of Neuber's method. One way of expressing the Neuber's rule is by Equation (18).

$$K_\sigma K_\varepsilon = K_T^2 \tag{18}$$

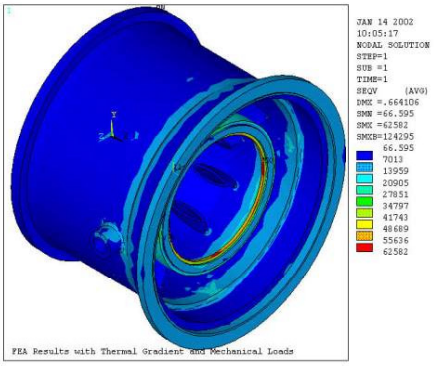

Figure 22. Equivalent Stress under Mechanical and Thermal Loading.

After utilizing the definition of stress and strain concentrations the final equation turns out to be:

$$\sigma.\varepsilon = Cons\tan t. \tag{19}$$

Equation (19) represents a hyperbola called Neuber's hyperbola. The intersection of this hyperbola and the stress-strain curve should provide the actual state of stress condition in the material (Figure 23). As indicated on the plot (Figure 20), the component has about 1000 life cycles.

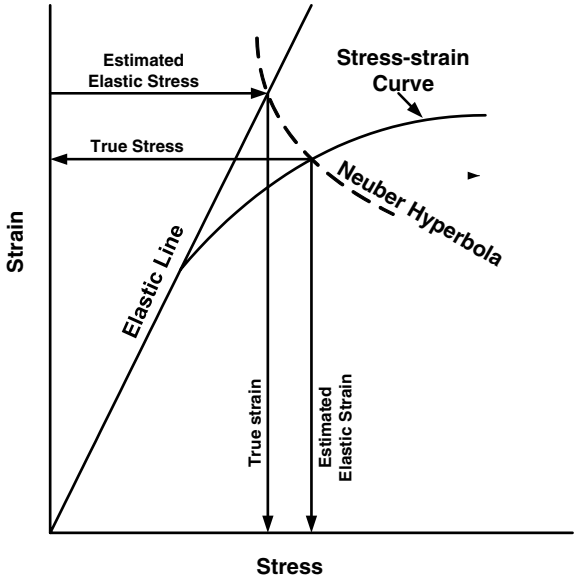

Figure 23. Depiction of Neuber's Hyperbola.

Results of a probabilistic calculation are discussed next. A variation of a total of about 10 percent is assumed for the strain amplitude; a 5 percent variation on both sides from the average value. Also a total of 5 percent variation in the material properties is assumed for the analysis. For this calculation only the plastic portion of the strain-life relation is utilized for simplicity. Figure (24) shows the plot of the probability for a given number of cycles.

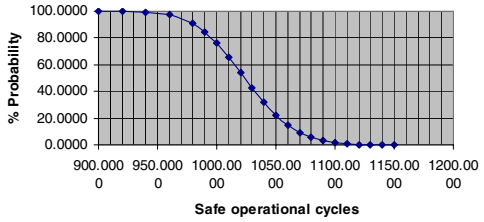

Figure 24. Safe Operational Cycle Versus Percent Probability.

There is about 79 percent probability for 1000 operational cycles. It seems that in this case 900 operational cycles seems to have nearly 100 percent probability.

EXAMPLE 3— RELIABILITY EVALUATION OF AN AXIAL COMPRESSOR DISK WITH INDICATION OF DISCONTINUITIES

Indications of crack like discontinuity were discovered on the rim of an axial compressor disk. A portion of the disk is shown in Figure 25. Analysis has been performed to determine the reliability of the disk and to find out whether it is suitable for long-term use. A linear elastic fracture mechanics (LEFM) approach was chosen to estimate reliability of the subject disk.

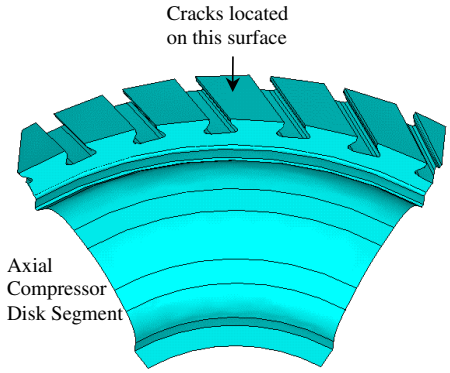

Figure 25. A Portion of Axial Compressor Disk.

Figure 26 shows the location of indications on the surface of the lock. To evaluate the effect of these on the reliability stress around these locations will be determined.

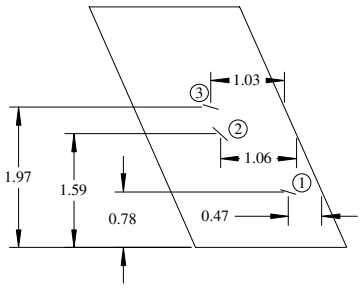

Figure 26. Location of Indications.

Stress levels were calculated by using finite element analysis. A "slice" of the disk representing one blade pitch was used for the analysis [Figure (27)]. To simulate the complete disk the displacement degrees of freedom of corresponding nodes of both surfaces of the "cut" sections were coupled. The blade centrifugal pull was simulated by applying loads equal to the centrifugal pull of the blade rotating at the maximum continuous operating speed of the compressor train.

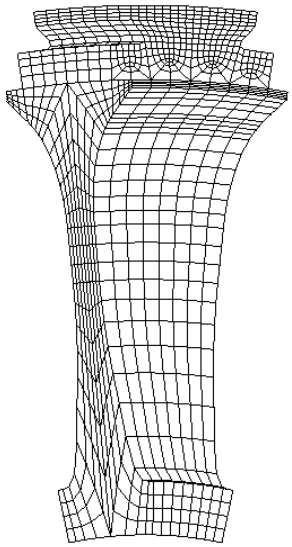

Figure 27. FE Model of One Pitch of the Disk.

After the analysis, the stress contours were plotted to determine the stress levels near the crack locations. As the following plots show, the indications are in areas where the stresses in planes perpendicular to the flaws are predominately compressive.

Figure 28 shows the tangential stress contours on the disk rim surface calculated at the maximum continuous operating speed (MCOS). Note that the stresses in the crack areas are predominately compressive. Based on classical analysis techniques, cracks located in elastic compressive stress fields should not propagate.

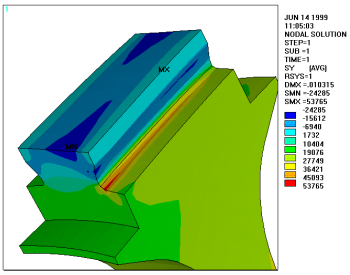

Figure 28. Tangential Stress Contour.

Figure 29 shows the axial stress contours on the disk rim surface at MCOS. Note that the stresses in the crack areas are predominately compressive. Any tensile stresses are very low.

Since it is difficult to determine the actual direction of growth of the crack tip, and since the direction of crack growth can change to conform to changing stress directions as the crack progresses, a conservative, but not unreasonable, approach to crack growth calculations is to use the maximum principal stress in the area of the cracks regardless of direction. The maximum principal stress contours in the areas of the indications are plotted in Figure 30 and Figure 31. Based on these plots it is evident that crack number 1 (Figure 26) is the most likely to progress to where it will break through the blade attachment wall.

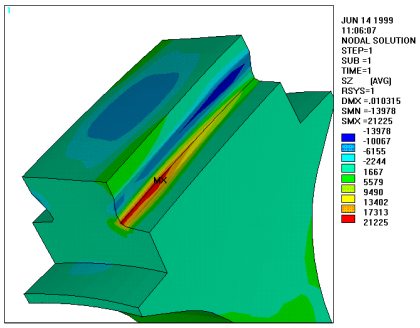

Figure 29. Axial Stress Contour.

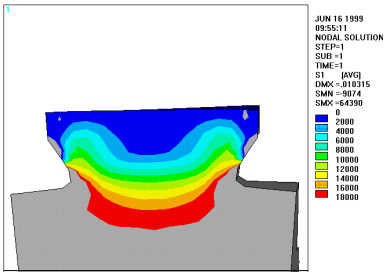

Figure 30. Maximum Principal Stress Contours at the Axial Midplane of the Disk. This Is near the Approximate Location of Cracks Nos. 2 and 3.

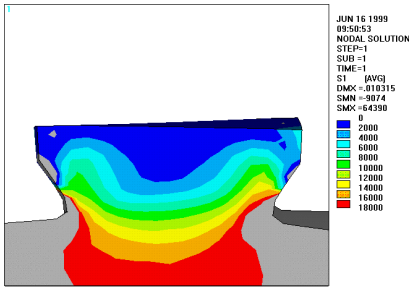

Figure 31. Maximum Principal Stress Contours in a Plane Through the Axial Location of Crack No. 1.

A stress of 14 ksi was chosen as the crack-tip stress for the crack growth calculations since it is the largest tensile principle stress in the crack area even though it is some distance from the crack tip and is oriented parallel to the plane of the crack.

The growth of crack number 1 will be used to estimate the suitability of the disk since that crack appears to be subjected to the highest maximum principle stress and is closest to the attachment. For this analysis, the length of crack number 1 is assumed to be 0.44 inch, the maximum length measured for these cracks.

DETERMINISTIC TYPE LEFM ANALYSIS

The first estimation is performed to see if the existing indications will grow in the first application of the load.

$$K_I = 1.3 * S(a)^{1/2}$$
$$K_I = 1.3 * 14(0.22)^{1/2} = 8.5\ ksi\left(sqrt(in)\right) \quad (20)$$

The calculated value of K_I is less than the material toughness, K_{Ic} [30 ksi (sqrt(in))], therefore the indication is not expected to be unstable in the first load application.

The next step in the analysis is to estimate the critical size of the growing crack. Size of the crack larger than the critical size will become unstable.

$$a_c = \left(K_{Ic} / (1.3 * S)\right)^2 \quad (21)$$

$a_c = (30 / (1.3*14))^2 = 2.7$ inches deep or 5.4 inches wide for semi-circular indication. This indicates that long before reaching the critical flaw size, crack number 1 will break into the blade attachment slot as shown in Figure 32. The crack size at breakthrough was estimated to be equal to 0.44 + 2 (0.25) = 0.94 inch.

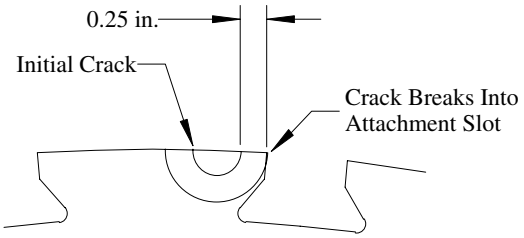

Figure 32. Possible Progression of Crack.

The next step in the analysis is to estimate the number of operational startup and shutdown cycles for initial indication to breakthrough into the attachment.

$$(da / dN) = 2.67 \times 10^{-11} (\Delta K)^{3.73} \quad (22)$$

As mentioned earlier in the "FRACTURE MECHANICS" section, Equation (22) should be numerically integrated. Assuming that the stress remains constant at the tip of the growing crack, the equation provided in the earlier section can be used. A numerical technique is used to calculate the number of cycles. The estimated number of operational cycles is 1.14E+06.

Based on the estimate, it will take more than 1.0 million start-stop cycles of the compressor for crack number 1 to breakthrough into the attachment.

PROBABILISTIC TYPE LEFM ANALYSIS

Each step described in the deterministic calculation will be repeated with utilizing the information about variation in the value used. For example, there is some inaccuracy in the determination of the indication size, material properties, and in the stress magnitude. For this example the following variations have been used:

- Stress varies between 13.3 ksi and 14.7 ksi, a total variation of 10 percent.
- Indication size between .418 and .462, 10 percent variation
- Material properties
- Fracture toughness, 30 ksi [sqrt(in)] to 43 ksi [(sqrt(in)]
  - b 3.534 to 3.912
  - m 2.40×10^{-11} to 2.94×10^{-11}

Results of this analysis are plotted in Figure 33 through Figure 35.

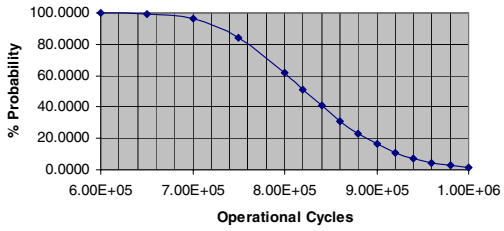

Figure 33. Safe Operational Cycle Versus Percent Probability.

Figure 33 is the plot of the probability of successfully achieving a desired operational cycle (start-stop). It is estimated that there is about 99.97 percent probability of achieving 6.00E+05 cycles while deterministic estimation of the cycle is 1.14E+06. The projected probability for the 1.14E+06 cycle is about 1.50 percent.

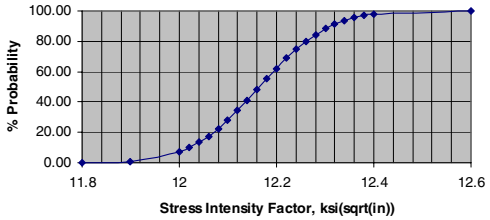

Figure 34. Magnitude of SIF Versus Percent Probability.

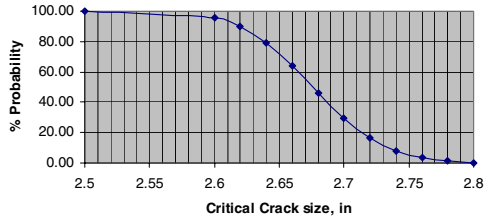

Figure 35.Critical Crack Size Versus Percent Probability.

Figure 34 is the plot of stress intensity factor (SIF) against its probability. This figure will help decide whether the crack will be unstable in the first application of load.

Figure 35 is the plot of critical crack size and its probability. The critical size of the crack becomes unstable. It shows that the critical size is about 2.5 inches with about 99.99 percent probability. The size of 2.7 inches calculated earlier from a deterministic analysis has a probability of about 29.5 percent.

EXAMPLE 4— FAILURE OF CRACKED COMPONENTS: FRACTURE MECHANICS APPROACH

The presence of a crack in a component may weaken it so that it fails by fracturing into two or more pieces. This can occur at stresses below the material's yield strength. The fracture mechanics approach was discussed earlier and the following example will demonstrate its use in evaluation of the reliability of a component.

Indications of crack like discontinuity were discovered near the blade slot (fir tree) of an expander disk shown in Figure 36. Linear elastic fracture mechanics was utilized to determine the suitability of its use. Stress levels were calculated using a detailed finite element model. For the purpose of this report the material properties were taken from those provided in *Aerospace Structural Metals Handbook* (1991). For example the following disk material properties for Waspaloy® at 800°F were used:

- Yield strength: YS = 106 ksi
- Fracture toughness: K_{IC} = 75 ksi $in^{1/2}$

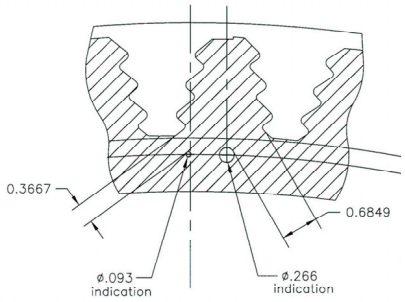

Figure 36. Expander Disk with Initial Cracks.

The crack growth rate was taken from published data (*Aerospace Structural Metals Handbook*, 1991) and is represented by the equation below (Figure 37):

$$(da/dN) = 3.96\times10^{-8}(\Delta K)^{1.821} \quad (23)$$

or

$$\log_{10}(da/dN) = 1.821\times\log_{10}(dK) - 7.402 \quad (24)$$

where:
da/dN = Crack growth rate, in/cycle
ΔK = Stress intensity at the crack tip point, ksi $in^{1/2}$

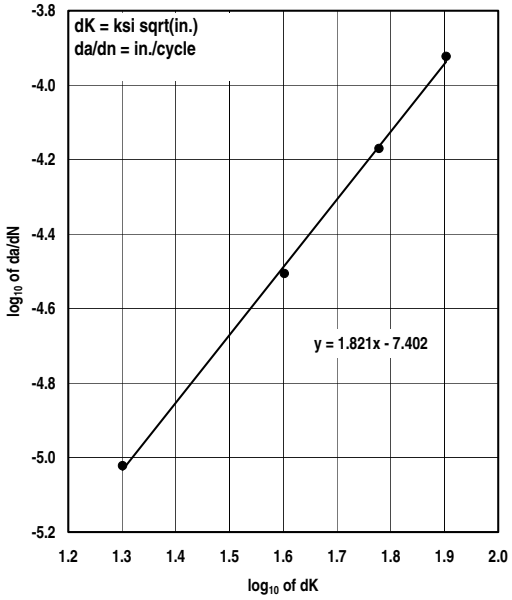

Figure 37. Plot Log (dK) Versus Log(da/dN) for Waspaloy® at 800°F.

A finite element analysis was performed to calculate stress levels. The FEA model for the blade and the detail of disk attachment area is shown in Figure 38. Stress levels in the area of the indications were taken from a solid (3-D) finite element stress analysis of a disk attachment under centrifugal loading at the rated speed of the expander. The centrifugal loading was assumed to be equal to the longest blade that can be utilized. The first principal stress at the indication location was the hoop stress (S) at 23.3 ksi.

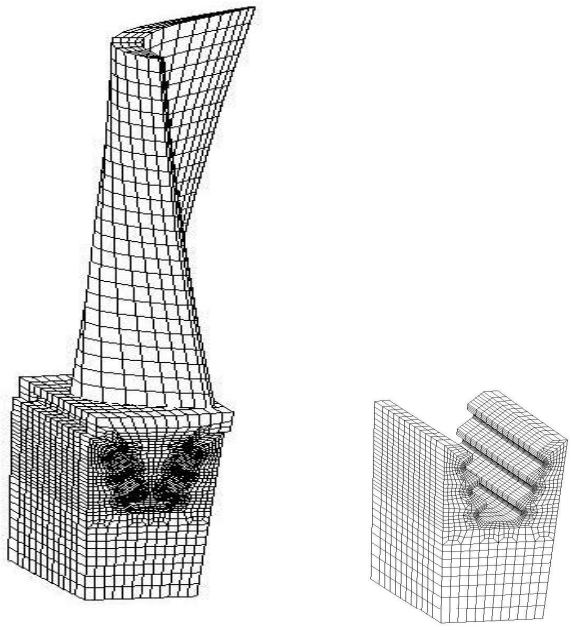

Figure 38. FEA Model of Blade and Attachments.

To help in the disposition of the disk the following two fracture mechanics evaluations were conducted.

- *Will the reported indication go to fracture in the first application of the load?* This is done by estimating the stress intensity factor and by comparing it to the fracture toughness of the material. This is similar to what was done in the previous example.

Diameter of the reported indication was 0.266 inches. The measured size of the indication was multiplied by 3.162 to simulate an area 10 times larger (assuming a circular indication). This was done to account for the inaccuracies in the measured areas of the indications. Therefore, for the evaluation, the initial flaw size (a) has been taken as 0.422 inch.

The following expression was used to estimate the stress intensity at the crack tip:

$$K_I = 1.12S(\pi a)^{1/2} = 1.12 \times 23.3(\pi 0.422)^{1/2} = 30.1 \; ksi \; in^{1/2} \quad (25)$$

Since, K_I (30.1 ksi $in^{1/2}$) < K_{IC} (75 ksi $in^{1/2}$), the indication will not become unstable in the first application of load.

- *How many start-stop cycles can the disk experience before the flaw sizes reach critical flaw size?* To be conservative, it was assumed that the indication spanned the bottom of the attachment for the entire thickness of the disk (about 4 inches). It was further assumed that the flaw spans to the attachment bottom.

This was done to add even more conservatism. It should be noted that the flaw being evaluated is not the size of the indication as reported but it was 0.6 inch deep over the entire thickness of the disk (about 4 inches).

The following expression was used to estimate the stress intensity at the crack tip:

$$\Delta K = 1.12 \times \Delta S(\pi a)^{1/2} \quad (26)$$

The calculated start-stop cycle is equal to 36,600 cycles.

The results of these two evaluations suggest that the disk is suitable for the intended application.

Similar to the previous example a probabilistic type calculation was performed. Variation in stress and material properties was assumed to be similar to the previous example.

Figure 39 is the plot of SIF against its probability. This figure will help decide whether the crack will be unstable in the first application of load. It shows that the value of SIF will have a range of 31 to 34 ksi [sqrt(in)]. Probability will have a range from 0.43 percent to 100 percent.

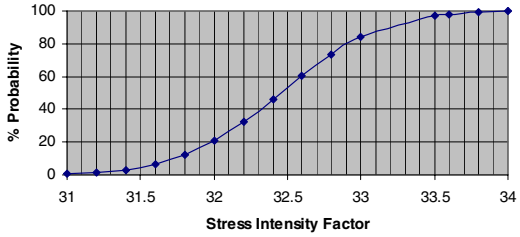

Figure 39. Stress Intensity Factor Versus Percent Probability.

Figure 40 is the plot of the probability of successfully achieving a desired operational cycle (start-stop). It is estimated that there is about 99.90 percent probability of achieving 36,000 cycles while deterministic estimation of the cycle is 36,600 cycles. The projected probability for the 36,600 cycle is about 99.00 percent.

SUMMARY

This paper focused on three points:

- Important modes of damage

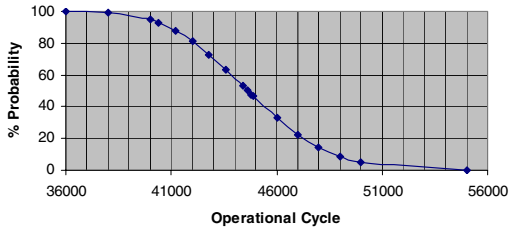

Figure 40. Operational Cycles Versus Percent Probability.

- Deterministic concept and factor of safety (factor of ignorance)
- Probabilistic concept and reliability

A discussion about basic modes contributing to the damage of mechanical components is provided. Concepts of damage with methods of its effect on the reliability of mechanical components have been presented. It is easier and it is a practice to make a decision based on deterministic concepts but it looks more real to make a decision based on probability/reliability/risk assessment. It is more honest to conduct a probabilistic type analysis. These will bring manufacturers and operators closer in realizing that there are always variations in the loads, geometry, and material properties so that a probabilistic type of analysis might provide a more realistic estimate of reliability or risk.

APPENDIX A— SOME OF THE THEORIES OF FAILURES WITH STATIC LOADS

Maximum Normal Stress Theory (Rankine Theory)

The material will fail under any condition of loading when the *maximum normal stress* at any point reaches the limiting value. Mathematically, this can be expressed as:

$$\sigma_u = S_m \quad (A\text{-}1)$$

where:
σ_u is the maximum principal stress
S_m is the limiting stress as determined from an axial test

Maximum Normal Strain Theory (Saint Venant Theory)

The material will fail at a point under any condition of loading when the *maximum normal strain* at that point reaches a critical value as determined for an axial test in tension or compression. Mathematically, this can be expressed as:

$$\varepsilon_u = \varepsilon_m \quad (A\text{-}2)$$

where:
ε_u is the maximum principal strain at the point
ε_m is the critical strain as determined from an axial test

Maximum Shearing Stress Theory
(A Special Case of Coulomb Theory)

Under any condition of loading, the material will fail when the maximum shear stress reaches the value of limiting shear stress as experimentally determined under pure shear test. Mathematically, this can be expressed as:

$$\sigma_{ij} = S_{mp} \quad (A\text{-}3)$$

where:
σ_{ij} is the maximum shear stress in the material
ε_m is the limiting shear stress determined from test

Maximum Shear Energy Theory
(Developed by Beltrami, Huber, Haigh)

The material will fail, regardless of the combination of stress and strain at the point when the value of strain energy per unit

volume at the point in the material reaches the maximum value of strain energy per unit volume that the material is capable of absorbing under an axial loading condition.

Strain Energy:

$$\begin{aligned} U_m &= S_{av}\varepsilon_{\max} \\ &= 1/2\ S_m\varepsilon_m \\ &= S_m^2/2E \\ &= E\ \varepsilon_m^2/2 \end{aligned} \tag{A-4}$$

The strain energy in a biaxial stress system per unit volume:

$$\begin{aligned} U &= \tfrac{1}{2}\ S_u\varepsilon_u + S_v\varepsilon_v \\ &= \tfrac{1}{2}\ S_u/E\left(S_u - vS_v\right) + \tfrac{1}{2}\ S_v/E\left(S_v - vS_u\right) \end{aligned} \tag{A-5}$$

or

$$U = 1/2E\left(S_u^2 - S_v^2 - 2vS_u^2S_v^2\right) \tag{A-6}$$

where:
u and v are two normal directions
v is Poisson's ratio

For the failure:

$$U = U_m \tag{A-7}$$

or

$$\left(S_u^2 - S_v^2 - 2vS_u^2S_v^2\right) = S_m^2 \tag{A-8}$$

Hencky vonMises Theory
(Developed by Hencky and vonMises Independently)

$$\left(S_u^2 - S_v^2\right) + \left(S_v^2 - S_w^2\right) + \left(S_w^2 - S_u^2\right) = 2S_m^2 \tag{A-9}$$

NOMENCLATURE

σ	psi	Stress
ε	in/in	Strain, subscript e for elastic, p for plastic, and t for total
σ_a	psi	Alternating stress
σ_e	psi	Fatigue strength
σ_m	psi	Mean stress
σ_{ult}	psi	Ultimate strength
$\Delta\varepsilon$	in/in	Strain range
$\Delta\sigma$	psi	Stress range
$\sigma_{f'}$	psi	Fatigue strength coefficient
C	None	Fatigue ductility coefficient
E	psi	Modulus of elasticity
FN	None	Factor of safety based on life
FS	None	Factor of safety based on stress
N_f	cycles	Cycles to failure
N_{f0}	cycles	Life when m = 0.0
N_{f1}	cycles	Life when FS = 1.0
b	None	Fatigue strength exponent
d	None	Fatigue ductility exponent
A	None	$\sigma_{f'}/E$ for zero mean stress
a,c	in	Crack dimensions
a_0	in	Starting crack dimension
a_c	in	Critical crack dimension
a_i	in	Starting crack dimension
a_f	in	Final crack dimension
a_{th}	in	Crack size that will not grow
K_{IC}	ksi	[sqrt(in)]Fracture toughness
K_I	ksi	[sqrt(in)] Stress intensity factor
K_T	None	Theoretical stress concentration
K_σ	None	Stress concentration
K_ε	None	Strain concentration
N	cycles-	Total number of cycles
ΔK_{th}	ksi[sqrt(in)]	Threshold value
P_f		Probability of failure

REFERENCES

Aerospace Structural Metals Handbook, 1991, Mechanical Properties Data Center, Columbus, Ohio: Battelle Columbus Laboratories.

"Characterization of Low Cycle High Temperature Fatigue by the Strainrange Partitioning Method," 1978, 46th Meeting of the AGARD Structures and Materials Panel, Aalbord, Denmark, AGARD-CP-243.

Coffin, L. F. Jr., 1971, "The Effect of Frequency on High-Temperature, Low-Cycle Fatigue," Proceedings of the Air Force Conference on Fatigue and Fracture of Aircraft Structures and Materials, AFFDL-TR-70-144, pp. 301-309.

Coffin, L. F., Jr., 1976, "The Concept of Frequency Separation in Life Prediction for Time-Dependent Fatigue," Symposium on Creep-Fatigue Interaction, R. M. Curran, Editor, MPC Publication No. 3, ASME, pp. 349-363.

Conway, J. B., Stentz, R. H., and Berling, J. T., 1975, "Fatigue, Tensile, and Relaxation Behavior of Stainless Steels," Published by Technical Information Center, Office of Information Services, U.S. Atomic Energy Commission.

Halford, G. R. and Manson, S. S., 1968, "Application of a Method of Estimating High-Temperature Low-Cycle Fatigue Behavior of Materials," Transactions of ASM, *61*, (1), pp. 94-102.

Herztberg, R.C., 1965, *Deformation and Fracture Mechanics of Engineering Materials*, New York, New York: John Wiley & Sons.

Hirakawa, K. and Tokimasa, K., 1981, "Creep-Fatigue Properties of Materials for High Temperature Service," The Sumitomo Search No. 26, pp. 118-135.

Larson, F. R. and Miller, J., 1972, Transactions of ASME, *74*, p. 765.

Leis, B. N., 1977, "An Energy-Based Fatigue and Creep-Fatigue Damage Parameter," *Journal of Pressure Vessel Technology*, *99*, (4), pp. 524-533.

Lucas, G. M. and Singh, M. P., 1992, "Compressed Air Energy Storage Design Challenges: LP Expander," *Power Generation Technology*.

Majumdar, S. and Maiya, P. S., 1979, "Creep-Fatigue Interactions in an Austenitic Stainless Steel," *Canadian Metallurgical*, *18*, (1), pp. 57-64.

Majumdar, S. and Maiya, P. S., 1976, "A Unified and Mechanistic Approach to Creep-Fatigue Damage," Second International Conference of Mechanical Behavior of Materials, American Society Metals. Also Argonne National Laboratory Report ANL-76-58.

Majumbar, S. and Maiya, P. S., 1980, "A Mechanistic Model for Time-Dependent Fatigue," *Journal of Engineering Materials Technology*, *102*, (1), pp. 159-167.

Manson, S. S., 1966, "Interface Between Fatigue, Creep, and Fracture," *International Journal of Fracture Mechanics*, *2*, (1), pp. 327-63.

Manson, S. S. and Halford, G. R., 1983, "Complexities of High Temperature Metal Fatigue—Some Steps Toward Understanding," NASA Technical Memo 83507.

Manson, S. S. and Halford, G. R., 1967, "A Method for Estimating High-Temperature Low-Cycle Fatigue Behavior of Materials," Proceedings of International Conference on Thermal and High-Strain Fatigue, The Metals and Metallurgy Trust, London, England, pp. 154-70.

Manson, S. S. and Halford, G. R., 1981, "Practical Implementation of the Double Linear Damage Rule and Damage Curve Approach for Treating Cumulative Fatigue Damage," *International Journal of Fracture Mechanics*, *17*, pp. 169-192.

Manson, S. S., Halford, G. R., and Hirschberg, M. H., 1971, "Creep-Fatigue Analysis by Strainrange Partitioning," *Design for Elevated Temperature Environment*, S. Y. Zamrik, Editor, ASME, pp. 12-24, discussion, pp. 25-28.

Manson, S. S., Halford, G. R., and Spera, D. A., 1971, "The Role of Creep in High Temperature Low-Cycle Fatigue," *Advances in Creep Design*, A. I. Smith and A. M. Nicholson, Editors, Halsted Press, pp. 229-249.

McKnight, R. L., Laflen, J. H., Halford, G. R., and Kaufman, A, 1983, "Turbine Blade Nonlinear Structural and Life Analysis," *Journal of Aircraft*, *20*, (5), pp. 475-480.

Moreno, V., Meyers, G. J., Kaufman, A., and Halford, G. R., 1983, "Nonlinear Structural and Life Analyses of a Combustor Liner," *Computers and Structures*, *16*, (1-4), pp. 509-515. Also NASA TM-82846, 1982.

Morrow, J., 1965, "Cyclic Plastic Strain Energy and Fatigue of Metals," ASTM STP 378, pp. 45-87.

Ostergren, W. J., 1976, "A Damage Function and Associated Failure Equations for Predicting Hold Time and Frequency Effects in Elevated Temperature Low Cycle Fatigue," *Journal of Testing and Evaluation*, *4*, (5), pp. 327-339.

Robinson, E. L., 1952, "Effect of Temperature Variation on the Long-Time Strength of Steels," Transactions of ASME, *74*, (5), pp. 777-80, discussion, pp. 780-81.

Schiffer, D., Singh, M. P., and Plummer, R., 1990, "Life Prediction of CAES L.P. Expander Components Using the Finite Element Technique," Life Assessment and Repair Technology—For Combustion Turbine Hot Section Components, Proceedings of an International Conference, Phoenix, Arizona.

Singh, M. P., 1985, "Turbine Blade Dynamics: A Probabilistic Approach," *Vibrations of Blades and Bladed Disk Assemblies*, ASME Book No. H000335, pp. 41-48.

Singh, M. P., 1991, "Reliability Evaluation of a Weld Repaired Steam Turbine Rotor Using Probabilistic Fracture Mechanics," PWR-13, *Design, Repair, and Refurbishment of Steam Turbines*, Book No. H00652, ASME.

Singh, M. P., 1992, "Predicting the Randomness of Forced Vibration Response of a Bladed Disc," ImechE Conference, Bath, United Kingdom, C432/128.

Singh, M. P., 2001, "Probabilistic HCF Life Estimation of a Mechanical Component," Proceeding of 2001 ASME International Mechanical Engineering Congress and Exposition, New York, New York.

Singh, M. P. and Ewins, D. J., 1988, "A Probabilistic Analysis of a Mistuned Bladed Turbine Disc," ImechE Conference, Edinburgh, United Kingdom, C229/88.

Singh, M. P., Sullivan, W. E., Donald G., and Hudson, J., 2004, "Probabilistic Life Assessment of an Impeller with Discontinuities," *Proceedings of the Thirty-Third Turbomachinery Symposium*, Turbomachinery Laboratory, Texas A&M University, College Station, Texas, pp. 15-23.

Taira, S., 1962, "Lifetime of Structures Subjected to Varying Load and Temperature," *Creep in Structures*, N. J. Hoff, Editor, Berlin, Germany: Springer Verlag, pp. 96-119, discussion, pp. 119-124.

Thacker, B. H., McClung, R. C., and Millwater, H. R., 1990, "Application of the Probabilistic Approximate Analysis Method to a Turbopump Blade Analysis," ASME 31st SDM Conference, Long Beach, California.

Viswanathan, R., Undated, "Damage Mechanisms and Life Assessment of High Temperature Components," ASM International, Metal Park, Ohio.

Vogel, W. H., Soderquist, R. W., and Schlein, B. C., 1976, "A Method for the Prediction of Crack Initiation Life in Combustor Chamber Liners," AIAA Paper No. 76-681, Presented at the AIAA/SAE 12th Propulsion Conference, Palo Alto, California.

ACKNOWLEDGMENTS

The authors would like to thank Chris Berger for encouragement and Mike Drosjack for valuable suggestions in preparation of the manuscript.